Research Square

Preprints are preliminary reports that have not undergone peer review.
They should not be considered conclusive, used to inform clinical practice,
or referenced by the media as validated information.

# Rational Design and Antibacterial Evaluation of Salicylideneaniline Schiff Bases Supported by Spectroscopic, Docking, and ADMET Analyses

**Saida Seridi**

seridi.saida@univ-guelma.dz

University of Guelma

**Sana Almi**

University of Biskra

**Ahmed LOUAFI**

University of Biskra

**Manal Chettibi**

University of Guelma

**Research Article**

**Keywords:**

**Posted Date:** September 1st, 2026

**DOI:** https://doi.org/10.21203/rs.3.rs-10765171/v1

**License:** This work is licensed under a Creative Commons Attribution 4.0 International License.
Read Full License

**Additional Declarations:** No competing interests reported.

# Abstract

In this study, two salicylideneaniline Schiff bases, 2-(((3-methoxyphenyl)imino)methyl)phenol (MMPIMP) and 2-(((2 methoxyphenyl)imino)methyl)phenol (OMPIMP), were synthesized via a simple condensation reaction and characterized by FT-IR and $^1$H NMR spectroscopy. Their antibacterial activity was assessed in vitro against *Staphylococcus aureus*, *Escherichia coli*, and *Pseudomonas aeruginosa* using disk diffusion and broth dilution assays. OMPIMP exhibited pronounced bactericidal effects against *E. coli* and *P. aeruginosa*, whereas MMPIMP showed primarily bacteriostatic activity, notably against *S. aureus*. Molecular docking revealed strong binding affinities of both compounds to *S. aureus* dihydrofolate reductase (DHFR), suggesting a potential mechanism of action. In silico ADMET predictions indicated excellent intestinal absorption, moderate clearance, absence of hepatotoxicity, and favorable safety profiles. Collectively, these results highlight OMPIMP, in particular, as a promising scaffold for developing new antibacterial agents to combat resistant bacterial strains.


# 1. Introduction

Combining chemical elegance with functional efficiency, Schiff bases occupy a pivotal position in modern scientific research. Their characteristic structure, dominated by an imine bond (-C = N-), endows them with remarkable versatility, opening the door to diverse applications in biological and chemical sciences. These compounds, formed by the reaction between a primary amine and a carbonyl compound, represent a class of molecules capable of addressing complex challenges with unparalleled flexibility [1–4].

In the biological field, they stand out for their impressive pharmacological activity, ranging from antibacterial and antifungal properties to antitumor and antiviral effects [5–13]. Their ability to interact with critical biomolecules, such as enzymes and DNA, offers promising perspectives for the development of new therapeutic agents, particularly in the face of increasing antibiotic resistance [14, 15]. Notably, Schiff bases have demonstrated antibacterial efficacy against Gram-positive and Gram-negative bacteria, sometimes surpassing standard antibiotics, as reported by Bayeh et al. (2020) [16]. Furthermore, molecular docking studies, as highlighted by Latif et al. (2023), reveal their ability to effectively interact with bacterial proteins, enhancing their antimicrobial potential [4].

Schiff bases play a crucial role in various fields beyond their medical applications. In analytical chemistry, they are widely used as chemical sensors for detecting metal cations and anions. For example, Schiff bases derived from orthophenylenediamine have been developed for the selective detection of $Cu^{2+}$ and $Zn^{2+}$ ions, offering high sensitivity and rapid colorimetric detection [17].

In materials science, Schiff bases serve as precursors for the synthesis of functional materials. Their versatile structure allows the formation of metal complexes with enhanced catalytic properties, facilitating critical processes for energy conversion. For instance, modified Schiff base complexes have been used for the direct catalytic conversion of $CO_2$ into formate, demonstrating efficiency comparable to the best-known nanocatalysts [18].

Additionally, metal complexes derived from Schiff bases are employed in catalysis for various reactions, including hydrogenation and oxidation, playing a crucial role in processes such as energy conversion and chemical synthesis [19].

This article aims to inspire deeper reflection on Schiff bases as key compounds capable of revolutionizing not only the treatment of resistant bacterial infections but also addressing critical needs across various industrial sectors. Their potential, at the intersection of chemistry and biology, paves the way for scientific innovations with significant practical applications.

## 2. Methodology

# 2.1. Synthesis of a Schiff Bases

The Schiff bases used in this study were synthesized through a conventional approach [20]. This process involved a direct condensation reaction in refluxing ethanol, utilizing an equimolar mixture (0.5 mol) of salicylaldehyde and the corresponding aniline (Fig. 1).

The reaction mixture was kept under reflux with magnetic stirring for approximately two hours. After the reaction was completed, the mixture was allowed to cool to room temperature, washed several times with ethanol, and then concentrated by removing the solvent using a rotary evaporator. The resulting solid products were purified through recrystallization in absolute ethanol, and their purity was verified using Thin Layer Chromatography (TLC).

The prepared Schiff bases were further characterized using infrared spectroscopy, electronic spectroscopy, and proton nuclear magnetic resonance ($^1$H-NMR) [21].

# 2.2. Antibacterial Activity of Schiff Bases

The synthesized compounds were screened for antibacterial activity against three representative strains: the Gram-negative *Escherichia coli* and *Pseudomonas aeruginosa*, and the Gram-positive *Staphylococcus aureus*. Using a standard disk diffusion assay, compounds dissolved in DMSO were applied to sterile disks on inoculated agar plates. Antibacterial potency was quantified by measuring the zones of inhibition around the disks after incubation.

## 3. Results and discussion

# 3.1 FT-IR Spectra

The infrared spectra of the synthesized Schiff bases were acquired utilizing KBr pellets with a Fourier transform spectrophotometer (SHIMADZU model FTIR-8400S) within the range of 400 $cm^{-1}$ to 4000 $cm^{-1}$, which corresponds to the vibrational energy spectrum of molecules. To aid visual interpretation,

the experimental IR spectrum of the compounds is displayed in Fig. 2. The spectra exhibit the subsequent distinctive bands:

- **- O-H stretching vibration**: The O-H stretching vibration is typically observed in the range of 3200–3600 $cm^{-1}$ [21, 22]. This band appears at 3350 $cm^{-1}$ in MMPIMP and at 3345 $cm^{-1}$ in OMPIMP, with slightly greater intensity in MMPIMP due to stronger hydrogen bonding.
- - **C = N stretching vibration**: The expected C = N stretching vibration is found in the range of 1600–1650 $cm^{-1}$ [23]. This band is observed at 1625 $cm^{-1}$ in MMPIMP and 1628 $cm^{-1}$ in OMPIMP, confirming the presence of the imine functional group.
- - **C-H aromatic and aliphatic stretching vibrations**: These vibrations are typically present between 2800–3100 $cm^{-1}$ [24]. In MMPIMP, they appear at 2920 $cm^{-1}$, whereas in OMPIMP, they are seen at 2915 $cm^{-1}$.
- **- C-O stretching vibration**: The C-O stretching vibration is expected in the range of 1000–1300 $cm^{-1}$ [21]. In MMPIMP, this band is observed at 1245 $cm^{-1}$, while in OMPIMP, it appears at 1250 $cm^{-1}$.
- **- Aromatic ring stretching vibrations**: These vibrations generally appear between 1200–1650 $cm^{-1}$ [25, 26]. In MMPIMP, they are recorded at 1505 $cm^{-1}$, whereas in OMPIMP, they are found at 1510 $cm^{-1}$.

A summary of the experimental IR bands and their corresponding functional group assignments is given in Table 1:

Table 1
Infrared Spectral Data of the Synthesized Schiff Bases

| Vibration | Absorption Band ($cm^{-1}$) | MMPIMP | OMPIMP |
|---|---|---|---|
| O-H stretching vibration | 3200–3600 $cm^{-1}$ | 3350 $cm^{-1}$ | 3345 $cm^{-1}$ |
| C = N stretching vibration | 1600–1650 $cm^{-1}$ | 1625 $cm^{-1}$ | 1628 $cm^{-1}$ |
| C-H aromatic and aliphatic stretching vibrations | 2800–3000 $cm^{-1}$ | 2920 $cm^{-1}$ | 2915 $cm^{-1}$ |
| C-O stretching vibration | 1000–1300 $cm^{-1}$ | 1245 $cm^{-1}$ | 1250 $cm^{-1}$ |
| Aromatic ring stretching vibrations | 1400–1600 $cm^{-1}$ | 1505 $cm^{-1}$ | 1510 $cm^{-1}$ |
| Out-of-plane C-H aromatic vibration | 750–900 $cm^{-1}$ | 820 $cm^{-1}$ | 825 $cm^{-1}$ |

# 3.2 1H NMR spectra

The NMR spectra of the ligands (Fig. 3–4) were recorded using deuterated dimethyl sulfoxide (or chloroform) as the solvent with a Bruker spectrometer (300 MHz).

The spectra of MMPIMP and OMPIMP show a singlet peak at 3.9 ppm, corresponding to the three protons of the O-$CH_3$ group. A multiplet around 7 ppm corresponds to the protons of the ortho-substituted benzene ring. For the other two compounds, a multiple in the 6.8–7.7 ppm range is observed, corresponding to the protons of the ortho- and meta-substituted benzene ring. The peak at 8.6 ppm corresponds to the proton of the CH = N group, while the peak at 13.6 ppm corresponds to the aromatic OH group.

Table 2 summarizes the main characteristic peaks of each synthesized compounds.

Table 2
$^1$H NMR Spectral Data of the Synthesized Schiff Bases.

| Schiff Base | δ (ppm) | Integration | Multiplicity |
|---|---|---|---|
| MMPIMP | 6.8–7.7 | 4 | m |
| | 3.9 | 4 | d |
| OMPIMP | 6.8–7.7 | 4 | m |
| | 3.9 | 2 | s |
| | 8.7 | 6 | s |
| | 14 | 7 | s |

# 3.3 Antibacterial activity

After 24 hours of incubation at 37°C, the antimicrobial sensitivity was determined by measuring the inhibition zone diameters.

The results are compiled in the Table 3.

- Negative control = DMSO (Inactive solvent).
- Positive control = Cefotaxime (CTX) 3 mg/mL.

According to the standardization of antibacterial activity [27], a strain is considered resistant or non-sensitive when the inhibition diameter is less than 8 mm. Diameters ranging from 9 to 14 mm indicate sensitivity, while those between 15 and 19 mm correspond to a very sensitive response. Finally, inhibition zones greater than 20 mm reflect an extremely sensitive strain.

The results obtained show that the tested Schiff bases exhibit varying antibacterial activities depending on the targeted bacterial strain. Cefotaxime (CTX) at 3 mg/mL (T+), used as the reference antibiotic, demonstrates very strong inhibitory activity (+++) against *Staphylococcus aureus* (36 mm), *Escherichia coli* (40 mm), and *Pseudomonas aeruginosa* (21 mm), confirming its broad-spectrum efficacy. In contrast, DMSO (T-), used as a solvent, exhibits no activity against the three tested strains, confirming its lack of antibacterial effect and its neutrality in compound evaluation. The Schiff bases OMPIMP and MMPIMP

show significant activity against *S. aureus*, with inhibition diameters of 22 mm and 16 mm at 20 µL, increasing to 26 mm and 23 mm at 30 µL, indicating dose-dependent efficacy (+++). However, against *E. coli*, OMPIMP exhibits weak inhibition (9 mm at 30 µL, +), while MMPIMP remains almost inactive (2 mm at 30 µL, -). Regarding *P. aeruginosa*, only MMPIMP shows slight activity (+), with inhibition zones of 7 mm at 20 µL and 10 mm at 30 µL.

This study shows that these substituted products exhibit an antibacterial effect against both Gram-positive and Gram-negative bacteria. It also indicates the ability of these synthetic compounds to penetrate the lipid membrane and target the organism to inhibit bacterial growth. Given their lipophilic nature (insoluble in water), they can solubilize within the membrane.

Table 3
Antibacterial activity of Schiff Bases:

| **Compound** | **Antibacterial activity (diameter (mm))** | | | | | | | | |
|---|---|---|---|---|---|---|---|---|---|
| | **Staphylococcus aureus** | | | **Escherichia coli** | | | **Pseudomonas aeruginosa** | | |
| | **20 µl** | **30 µl** | **Strain Category** | **20 µl** | **30 µl** | **Strain Category** | **20 µl** | **30 µl** | **Strain Category** |
| OMPIMP | 22 | 26 | +++ | 0 | 9 | + | - | - | - |
| MMPIMP | 16 | 23 | +++ | 0 | 2 | - | 7 | 10 | + |
| T+ | 36 | - | +++ | 40 | - | +++ | 21 | - | +++ |
| T- | 0 | - | - | 0 | - | - | 0 | - | - |

The histogram shows that the Schiff bases (OMPIMP and MMPIMP) exhibit varying antibacterial activity against *Staphylococcus aureus*, *Escherichia coli*, and *Pseudomonas aeruginosa*, with inhibition zone diameters suggesting differing effectiveness depending on the target bacteria, while the control (T) shows little to no activity. These results indicate that OMPIMP and MMPIMP could act as promising antibacterial agents, particularly against Gram-positive and Gram-negative strains, although *Pseudomonas aeruginosa*, known for its resistance, appears less susceptible. These findings highlight the need for further studies to assess their therapeutic potential and optimize their chemical structure.

# 3.4 Characterization of the Bacteriostatic or Bactericidal Effect

The bactericidal or bacteriostatic effect of the antibiotic was evaluated according to established standards: if the MBC is close to the MIC (MBC/MIC ratio of 1 or 2), the antibiotic is considered bactericidal. In contrast, if the MBC is significantly higher than the MIC (MBC/MIC ratio between 4 and 16), the antibiotic is considered bacteriostatic [28]. However, if the antibiotic is typically classified as bactericidal, and the MBC/MIC ratio falls within this higher range, the bacterial strain is considered tolerant.

## 3-4-1 Determination of MIC in liquid medium

MIC is determined using U-bottom 96-well microtiter plates. Each well is filled with 150 µL of nutrient broth. In well 1, 40 µL of an antibiotic solution (ligand) at 40 mg/mL is added. Serial two-fold dilutions are performed from well 1 to well 11, resulting in final concentrations ranging from 40 mg/mL to 0. Then, 5 µL of bacterial inoculum (0.5 McFarland standard) is added to each well. This method allows determination of the MIC for each tested product against three bacterial strains: *E. coli*, *P. aeruginosa*, and *S. aureus* (Fig. (6)).

## 3-4-2 Determination of MBC in solid medium:

Nutrient agar poured into Petri dishes is inoculated in series using the contents of tubes with concentrations equal to or greater than the MIC from the previous dilution series. The MBC is determined after 24 hours of incubation at 37°C.

The bacteriostatic or bactericidal effect was characterized by the MBC/MIC ratio, as shown in Table 4.

Table 4
The MIC and MBC values

| Strains | Products | MIC (mg/ml) | MBC (mg/ml) | MBC/MIC | Effect |
|---|---|---|---|---|---|
| **E.Coli ATCC 25922** | MMPIMP | 1 | > 8 | ND | Bacteriostatic |
| | OMPIMP | 2 | 8 | 4 | Bactericidal |
| **Pseud. aeruginosa ATCC 27853** | MMPIMP | 0.5 | 4 | 8 | Bacteriostatic |
| | OMPIMP | 2 | 4 | 2 | Bactericidal |
| **Sta. Aureus ATCC 25923** | MMPIMP | 0.25 | > 8 | ND | Bacteriostatic |
| | OMPIMP | 0.125 | 8 | 64 | Bacteriostatic |

The examination of the results indicates that the tested products, MMPIMP and OMPIMP, demonstrate differing antibacterial activity based on the bacterial strains examined. MMPIMP is predominantly bacteriostatic, impeding bacterial proliferation without a notable bactericidal impact. The minimum bactericidal concentration (MBC) of MMPIMP against E. coli and S. aureus surpasses 8 mg/ml, signifying an absence of direct lethal efficacy. Conversely, OMPIMP exhibits a bactericidal effect against E. coli and Pseudomonas aeruginosa, with an MBC/MIC ratio of < 4, indicating enhanced efficiency in eradicating these bacteria. Nonetheless, against S. aureus, OMPIMP retains its bacteriostatic properties despite a comparatively low MIC (0.125 mg/ml), signifying effective growth suppression without a rapid bactericidal effect. In comparing the effects on Gram-positive and Gram-negative bacteria, OMPIMP demonstrates greater efficacy against resistant Gram-negative pathogens, including P. aeruginosa and E.

coli, positioning it as a potentially valuable candidate for targeted antibacterial applications. Consequently, our findings indicate that OMPIMP may be utilised for the treatment of illnesses induced by Gram-negative bacteria, whilst MMPIMP could serve to restrict bacterial proliferation as an adjunct to a bactericidal agent.

## 3–5 Molecular docking simulation

Docking studies revealed how Schiff base compounds inhibit bacteria's growth by understanding its mechanism. The studies were done to evaluate the binding affinity of Schiff bases and their interactions with the target protein of Staphylococcus aureus [29]. We docked the ligand with the protein using AutoDock Vina [30] and visualized the protein-ligand complexes using the BIOVIA Discovery Studio [31].

The dihydrofolate reductase (DHFR) enzyme from Staphylococcus aureus is defined by the crystal structure code 2W9S. The structure was determined through X-ray diffraction at a resolution of 1.80 Å and is available from the [RCSB Protein Data Bank](https://www.rcsb.org/).

A hydrogen bond is formed between the hydroxyl group of OMPIMP and a SER49 residue. It is also worth noting that hydrophobic residues ILE50, LEU20 and ILE14 are present because of the aromatic rings [32] by binding energy − 8.1 kcal/mol.

MMPIMP is stabilized by docking scores of -7.6 kcal/mol. The hydroxyl group forms two hydrogen bonds with SER49 and ASN18. The methoxy group establishes one hydrogen bond and one hydrophobic interaction with ALA7, as well as two hydrophobic interactions with ILE14 and LEU20. Additionally, the aromatic rings create two hydrophobic interactions with the residues LEU20 and ILE50 [33].

In silico predictions for chosen targets revealed probable binding patterns within the active site, indicating that both ligands demonstrated increased antibacterial action against S. aureus.

## 3–6 ADMET and pharmacokinetics

ADMET plays a crucial role in pharmacokinetics, influencing the drug's absorption, distribution, metabolism, and excretion processes. Understanding these processes is essential for optimizing drug efficacy and minimizing toxicity in therapeutic applications[34]. Employing the computational frameworks provided by the pkCSM webserver[35] (https://biosig.lab.uq.edu.au/pkcsm/prediction) enables us to efficiently and precisely forecast these parameters.

## 3-6-1 Absorption

Enhancing absorption is vital for improving the bioavailability of drugs, especially those with poor membrane permeability, which can significantly impact therapeutic effectiveness. A drug with good absorption properties should have a medium to high rate of absorption, high cell membrane permeability,

and the ability to easily pass through biological membranes [36].An examination of the permeability data presented in Table 5revealed that the assessed molecules exhibited elevated Caco2 permeability values (range: 1.129–1.174) concomitantly with intestinal absorption ratios of approximately 94.21%, indicating a substantial capacity for absorption.

## 3-6-2 Distribution

The distribution of a drug within the body is equally important, as it determines the drug's availability at the site of action and influences overall therapeutic outcomes. The forecasted bio distribution of the two bioactive compounds yielded calculated blood-brain barrier (BBB) permeability values of 0.167 and 0.052, indicating a heightened likelihood of transverse blood-brain barrier penetration [37].

The permeability of the central nervous system (CNS), commonly referred to as LogPS, constitutes a critical parameter that quantifies the capacity of pharmacological agents to infiltrate the CNS; consequently, it is essential for the assessment of therapeutics aimed at the CNS[36] .The data presented in Table 5 revealed low LogPS values of -1.405 and − 1.417, indicating an inability to permeate the CNS, thereby mitigating the risk of any potential deleterious effects on the central nervous system.

## 3-6-3 Metabolism

Metabolism is the process by which the body breaks down substances [34], converting them into metabolites. Cytochrome P450 (CYP450) enzymes, specifically CYP2D6 and CYP3A4, are integral to the metabolic processing of pharmaceuticals, the detoxification of deleterious compounds, and a multitude of physiological mechanisms [38]. The results demonstrated that the compounds do not act as substrates or inhibitors for CYP-2D6 and CYP3A4.

## 3-6-4 Excretion

Excretion plays a crucial role in maintaining homeostasis, as it helps to remove potentially harmful substances and regulate the internal environment of the body. Clearance refers to the volume of plasma from which a substance is completely removed per unit time, reflecting the efficiency of excretion processes in the body [39]. The synthesized compounds exhibited moderate clearance rates, varying between 0.283 and 0.218, which fall within the acceptable thresholds for their retention capabilities.

## 3-6-5 Toxicity

Toxicity study is an essential component of drug development, as it evaluates the safety and adverse effects of substances on living organisms. it is essential to evaluate the prospective toxicity of the experimental compounds, as this factor markedly impacts the pharmacological selection process [40,

41]. It was established that all of the compounds demonstrated a favorable safety profile and were free from any deleterious effects, with the exception of AMES toxicity.

Table 5
ADMET properties of the synthesized compounds.

| Properties | MMPIMP | OMPIMP | Unit |
|---|---|---|---|
| Absorption | | | |
| Caco2 permeability | **1.129** | **1.174** | Numeric (log Papp in $10^{-6}$ cm/s) |
| Intestinal absorption (human) | **94.213** | **94.24** | Numeric (% Absorbed) |
| Distribution | | | |
| BBB permeability | **0.167** | **0.052** | Numeric (log BB) |
| CNS permeability | **-1.405** | **-1.417** | Numeric (log PS) |
| Metabolism | | | |
| CYP2D6 substrate | **No** | **No** | Categorical (Yes/No) |
| CYP3A4 substrate | **No** | **No** | Categorical (Yes/No) |
| CYP2D6 inhibitior | **No** | **No** | Categorical (Yes/No) |
| CYP3A4 inhibitior | **No** | **No** | Categorical (Yes/No) |
| Excretion | | | |
| Total Clearance | **0.283** | **0.218** | Numeric (log ml/min/kg) |
| Toxicity | | | |
| AMES toxicity | **Yes** | **Yes** | Categorical (Yes/No) |
| Hepatotoxicity | **No** | **No** | Categorical (Yes/No) |
| Skin Sensiisation | **No** | **No** | Categorical (Yes/No) |

## 3–7 Structural Insights from RDG Analysis of the Schiff Bases

The Reduced Density Gradient (RDG) analysis was performed using *Multiwfn* version 3.8 to visualize non-covalent interaction (NCI) patterns in the synthesized Schiff bases MMPIMP and OMPIMP. Although both molecules are structural isomers differing only in the position of the methoxy substituent on the aniline ring (meta for MMPIMP, ortho for OMPIMP), clear differences were observed in their interaction profiles.

For MMPIMP, the RDG plot highlights pronounced steric repulsion regions (red areas) around the aromatic rings and hydrogen atoms, indicative of a more rigid and compact molecular conformation. In

contrast, OMPIMP displays broader van der Waals interaction zones (green areas) and distinct attractive interaction regions (blue areas), particularly around the ortho-methoxy group. These blue zones suggest the presence of intramolecular hydrogen bonding or stabilizing dipole–dipole interactions, a behavior commonly reported for ortho-substituted Schiff bases [42, 43].

Such interactions enhance conformational flexibility and promote favorable molecular recognition with biological targets [44, 45]. These computational findings are consistent with the superior antibacterial activity observed experimentally for OMPIMP, illustrating how even a subtle positional change in a substituent can markedly influence the non-covalent interaction landscape and pharmacological performance [46].

## 4. Conclusion

The synthesized Schiff bases MMPIMP and OMPIMP exhibit significant potential as antibacterial agents, with OMPIMP demonstrating strong bactericidal effects against Gram-negative bacteria. Spectroscopic characterization confirmed the successful formation of the imine linkage, and biological evaluations highlighted their differential activity against diverse bacterial strains. Molecular docking studies revealed strong interactions with bacterial DHFR, supporting their mechanism of action at the molecular level. Additionally, favorable ADMET properties—including high absorption, low toxicity, and non-inhibition of major CYP450 enzymes—reinforce their drug-likeness and therapeutic promise. Overall, this study not only underscores the value of salicylideneaniline derivatives in antibacterial research but also paves the way for further in vivo investigations and structure–activity optimization to enhance their pharmacological efficacy.

## Declarations

# Funding

The authors declare that no funds, grants, or other financial support were received for the research, authorship, or publication of this manuscript.

# Author Contribution

S.Seridi wrote the main manuscript textS.Almi prepared 2.1. Synthesis of a Schiff Bases and characterizedA. Louafi prepared Antibacterial Activity M.Chettibi prepared 3-5 Molecular docking simulation

## References

1. Tian YP, Duan CY, You XZ, Pahontu E, Julea F, Rosu T, Purcarea V, Chumakov Y, Petrenco P, Gulea A (1997) vol. 23, p. 17 https://doi.org/10.1023/A:1006937413506. 2. X. Zhu, C. Wang, and Z. Lu,

*Transit. Met. Chem.*, 1997, vol. 22, p. 9. https://doi.org/10.1023/A:1018453316348 3. E. Pahontu, F. Julea, T. Rosu, V. Purcarea, Y. Chumakov, P. Petrenco, A. Gulea *Willey, J. Cell. Mol. Med.*, 2015, vol. 19, p. 865. https://doi.org/10.1111/jcmm.12508

2. Latif MA, Ahmed T, Hossain MS, Chaki BM (2023) A. Abdo*c*, and Md. Kudrat-E-Zahan, Synthesis, Spectroscopic Characterization, DFT Calculations, Antibacterial Activity, and Molecular Docking Analysis of Ni(II), Zn(II), Sb(III), and U(VI) Metal Complexes Derived from a Nitrogen-Sulfur Schiff Base, Russian Journal of General Chemistry, Vol. 93, No. 2, pp. 389–397. 10.1134/S1070363223020214
3. Murtaza G, Mumtaz A, Khan FA, Ahmad S, Azhar S, Najam-Ul-Haq M, Atif M, Khan SA, Maalik A, Alam F, Hussain I, Recent pharmacological advancements in Schiff bases: A review., Antony 7R, Arun T, Manickam STD, Pund AA, Saboo SS, Sonawane GM, Dukale AC, Magare BK (2014) 6. T.F.F. Magalhães, C.M. da Silva, L.B.F. dos Santos, D.A.Santos, L.M. Silva, B.B. Fuchs, E. Mylonakis, C.V.B. Martins, M.A. Resende Stoianoff, and Â. de Fátima, Cinnamyl Schiff bases: synthesis, cytotoxic effects and antifungal activity of clinical interest. *Lett. Appl. Microbiol*., 71 (5): 490–497 (2020). https://doi.org/10.1111/lam.13356 7. R. Antony, T. Arun, S.T.D. Manickam, A review on applications of chitosan-based Schiff bases. *Int. J. Biol. Macromol.*, 129: 615–633 (2019) https://doi.org/10.1016/j.ijbiomac.2019.02.047. 8. I. Ledeţi, A. Alexa, V. Bercean, G.Vlase, T.V lase, L.-M. Şuta, and A. Fuliaş, Synthesis and degradation of Schiff bases containing heterocyclic pharmacophore. *Int. J. Mol. Sci.*, 16: 1711–1727 (2015). https://doi.org/10.3390/ijms16011711 9. A.A. Pund, S.S. Saboo, G.M. Sonawane, A.C. Dukale, B.K. Magare Synthesis of 2,5-disubstituted-1,3,4-thiadiazole derivatives from (2*S*)-3-(benzyloxy)-2-[(tertbutoxycarbonyl) amino] propanoic acid and evaluation of anti-microbial activity. *Synth Commun*., https://doi.org/10.1080/00397911.2020.1817488
4. Morsy NM, Hassan AS, Hafez TS, Mahran MRH, Sadawe IA, Gbaj AM (2021) Synthesis, antitumor activity, enzyme assay, DNA binding and molecular docking of *Bis*-Schiff bases of pyrazoles. J Iran Chem Soc 18(1):47–59. https://doi.org/10.1007/s13738-020-02004-y
5. Sztanke K, Maziarka A, Osinka A, Sztanke M, An insight into synthetic Schiff bases revealing antiproliferative activities (2013) http://dx.doi.org/10.1016/j.bmc.2013.04.037 12. A.S. Hassan, A.A. Askar, A.M. Naglah, Almehizia, A.A. and Ragab, A., Discovery of new Schiff bases tethered pyrazole moiety: Design, synthesis, biological evaluation, and molecular docking study as dual targeting DHFR/DNA gyrase inhibitors with immunomodulatory activity. *Molecules*, 25 (11): 2593 (2020) https://doi.org/10.3390/molecules25112593
6. Mukhtara SS, Hassana AS, Morsya NM, Hafeza TS, Hassaneenb HM, Saleh FM (2021) Overview on Synthesis, Reactions, Applications, and Biological Activities of Schiff Bases. Egypt J Chem Vol 64(11):6541–6554. 10.21608/ejchem.2021.79736.3920
7. P.Rao, - A Review on Versatile Applications of Novel Schiff Bases and Their Metal Complexes (2019) Lett Appl Nanobiosci 8(4):675–681. https://doi.org/10.33263/LIANBS84.675681
8. Golcu A, Tumer M, Demirelli H, Wheatley A (2005) Cd(II) and Cu(II) Complexes of Polydentate Schiff Base Ligands: Synthesis, Characterization, Properties and Biological Activity. Inorg Chim Acta

358(6):1785–1797. https://doi.org/10.1016/j.ica.2004.11.026

9. Bayeh Y, Mohammed F, Gebrezgiabher M, Elemo F, Getachew M, Thomas M (2020) - Synthesis, Characterization and Antibacterial Activities of Polydentate Schiff Bases, Based on Salicylaldehyde. Adv Biol Chem 10(5):127–139. https://doi.org/10.4236/abc.2020.105010
10. Ejiah FN, Rofiu MO, Oloba-Whenu OA, Fasina TM (2023) Schiff bases as analytical tools: synthesis, chemo-sensor, and computational studies of 2-aminophenol Schiff bases. Mater Adv 4:2308–2321. 10.1039/D3MA00097D
11. Liu Q, Yang X, Li L, Miao S, Li Y, Li Y, Wang X, Huang Y, Zhang T Direct catalytic hydrogenation of $CO_2$ to formate over a Schiff-base-mediated gold nanocatalyst, *nature communications* | 8: 1407 | 10.1038/s41467-017-01673-3
12. Liu X, Manzur C, Novoa N, Hamon JR (2018) Multidentate unsymmetrically-substituted Schiff bases and their metal complexes: Synthesis, functional materials properties, and applications to catalysis. Coord Chem Rev 357:144–172. https://doi.org/10.1016/j.ccr.2017.11.030
13. Patel MN, Patel CB, Patel RP (1974) Chelates of Cu(II) with Some Bidentate Schiff Bases. 36:3868–3870. 10.1016/0022-1902(74)80186-7. Journal of Inorganic and Nuclear Chemistry
14. Benmabrouk M, Seridi S, Aimene Y, Almi S (2023) Synthesis, Spectroscopic Characterization, DFT, and Molecular Docking Analysis of Some Salicylideneaniline Schiff Base Derivatives as Potential Antioxidant Compounds. Polycycl Aromat Compd. 10.1080/10406638.2023.2276252
15. Reichenb €acher M, Popp J (2012) Challenges in Molecular Structure Determination. Springer Science & Business Media, Berlin
16. Gao X, Wen X, Esser L, Quinn B, Yu L, Yu CA, Xia D (2003) Structural Basis for the Quinone Reduction in the bc1 Complex: A Comparative Analysis of Crystal Structures of Mitochondrial Cytochrome bc1 with Bound Substrate and Inhibitors at the Qi site. Biochemistry 42(30):9067–9080. 10.1021/bi0341814
17. Maghraoui N, Aggoun D, Bouzerafa B, Bezzi H, Ouennoughi Y, López D, García MF, Ourari A, Mubarak MS (2021) Synthesis, characterization, thermal stability, electrochemical behavior, and antioxidant activity of new oxovanadium(iv) and iron(ii) tetradentate Schiff base complexes. Arab J Chem 14:103025. https://doi.org/10.1016/j.arabjc.2021.103025
18. Sathyanarayana DN (2015) Vibrational Spectroscopy: Theory and Applications. New Age International, New Delhi
19. € Yıldırım AO, Yıldırım MH (2022) Kas ¸tas, Synthesis, Spectroscopic, Conceptual DFT Characterization and Molecular Docking Studies of Two Versatile di-Bromobenzaldehyde Derived Compounds. Polycycl Aromat Compd 42:8: 5599–5615. 10.1080/10406638.2021.1946095
20. Bouharb H, El Badaoui K, Zair T, El amri J, Alaoui SC (2014) Selection of Some Medicinal Plants from Zerhoun (Central Morocco) for Antibacterial Activity Against *Pseudomonas aeruginosa*. J Appl Biosci 78:6685–6693
21. *X.* CLSI. Methods for Dilution Antimicrobial Sucseptibility Tests for Bacteria That Grow Aerobically. 8. Clinical and Laboratory Standards Institute; Wayne, PA: (2009)

22. Zimmermann S et al (Dec. 2019) Clinically Approved Drugs Inhibit the Staphylococcus aureus Multidrug NorA Efflux Pump and Reduce Biofilm Formation. Front Microbiol 10:2762. 10.3389/fmicb.2019.02762
23. 'Evaluation of AutoDock and AutoDock Vina on the CASF -2013 Benchmark | Journal of Chemical Information and Modeling'. Accessed: May 27, 2025. [Online]. Available: https://pubs.acs.org/doi/abs/10.1021/acs.jcim.8b00312
24. Baroroh U, Si. S, Biotek. M, Muscifa ZS, Destiarani W, Rohmatullah FG, Yusuf M (2023) 'Molecular interaction analysis and visualization of protein-ligand docking using Biovia Discovery Studio Visualizer', *IJCB*, vol. 2, no. 1, p. 22. 10.24198/ijcb.v2i1.46322
25. Ikram M et al (Sep. 2023) Graphitic-carbon nitride and poly acrylic acid doped vanadium oxide for efficient catalytic and antimicrobial activity: In silico molecular docking studies. J Photochem Photobiol A 443:114835. 10.1016/j.jphotochem.2023.114835
26. K R, Kakkassery JT, Raphael VP, Johnson R, K VT (2021) 'In vitro antibacterial and in silico docking studies of two Schiff bases on Staphylococcus aureus and its target proteins', *Futur J Pharm Sci*, vol. 7, no. 1, p. 78, Dec. 10.1186/s43094-021-00225-3
27. Chandrasekaran B, Abed SN, Al-Attraqchi O, Kuche K, Tekade RK (2018) Computer-Aided Prediction of Pharmacokinetic (ADMET) Properties. Dosage Form Design Parameters. Elsevier, pp 731–755. doi: 10.1016/B978-0-12-814421-3.00021-X.
28. Pires DEV, Blundell TL, Ascher DB (May 2015) pkCSM: Predicting Small-Molecule Pharmacokinetic and Toxicity Properties Using Graph-Based Signatures. J Med Chem 58(9):4066–4072. 10.1021/acs.jmedchem.5b00104
29. Flores-Holguín N, Frau J, Glossman-Mitnik D (Aug. 2021) In Silico Pharmacokinetics, ADMET Study and Conceptual DFT Analysis of Two Plant Cyclopeptides Isolated From Rosaceae as a Computational Peptidology Approach. Front Chem 9:708364. 10.3389/fchem.2021.708364
30. Lagorce D, Douguet D, Miteva MA, Villoutreix BO (Apr. 2017) Computational analysis of calculated physicochemical and ADMET properties of protein-protein interaction inhibitors. Sci Rep 7(1):46277. 10.1038/srep46277
31. Veith H et al (2009) 'Comprehensive characterization of cytochrome P450 isozyme selectivity across chemical libraries', *Nat Biotechnol*, vol. 27, no. 11, pp. 1050–1055, Nov. 10.1038/nbt.1581
32. Zakharov AV, 'Computational Tools And Resources For Metabolism-Related Property Predictions (2012). 2. Application To Prediction Of Half-Life Time In Human Liver Microsomes', *Future Medicinal Chemistry*, vol. 4, no. 15, pp. 1933–1944, Oct. 10.4155/fmc.12.152
33. Blomme EAG, Will Y (Apr. 2016) Toxicology Strategies for Drug Discovery: Present and Future. Chem Res Toxicol 29(4):473–504. 10.1021/acs.chemrestox.5b00407
34. extension://efaidnbmnnnibpcajpcglclefindmkaj /https://pharmabookbank.wordpress.com/wp-content/uploads/2019/03/2.burgers_medicinal-chemistry-vol-2-.pdf. (n.d.)
35. Johnson ER, Keinan S, Mori-Sánchez P, Contreras-García J, Cohen AJ, Yang W (2010) Revealing Noncovalent Interactions. J Am Chem Soc 132(18):6498–6506. https://doi.org/10.1021/ja100936w

36. Contreras-García J, Johnson ER, Keinan S, Chaudret R, Piquemal JP, Beratan D, Yang W (2011) NCIPLOT: A Program for Plotting Noncovalent Interaction Regions. J Chem Theory Comput 7(3):625–632. https://doi.org/10.1021/ct100641a
37. Tolstoy PM, Filarowski A (2016) Some Brief Notes on Theoretical and Experimental Investigations of Intramolecular Hydrogen Bonding in Ortho-Hydroxyaryl Schiff Bases. Molecules 21:1657. https://doi.org/10.3390/molecules21121657
38. Panek JJ, Filarowski A (2019) Intramolecular Hydrogen Bonds in Selected Aromatic Compounds. Catalysts 9(11):909. https://doi.org/10.3390/catal9110909
39. Verma D, Sharma S, Vashishtha M (2023) Evaluation of Molecular Structure-Antimicrobial and Antioxidant Efficacy Relationship of Schiff Bases. Environ Sci Pollut Res 30:20874–20886. https://doi.org/10.1007/s11356-022-23633-1

## Figures

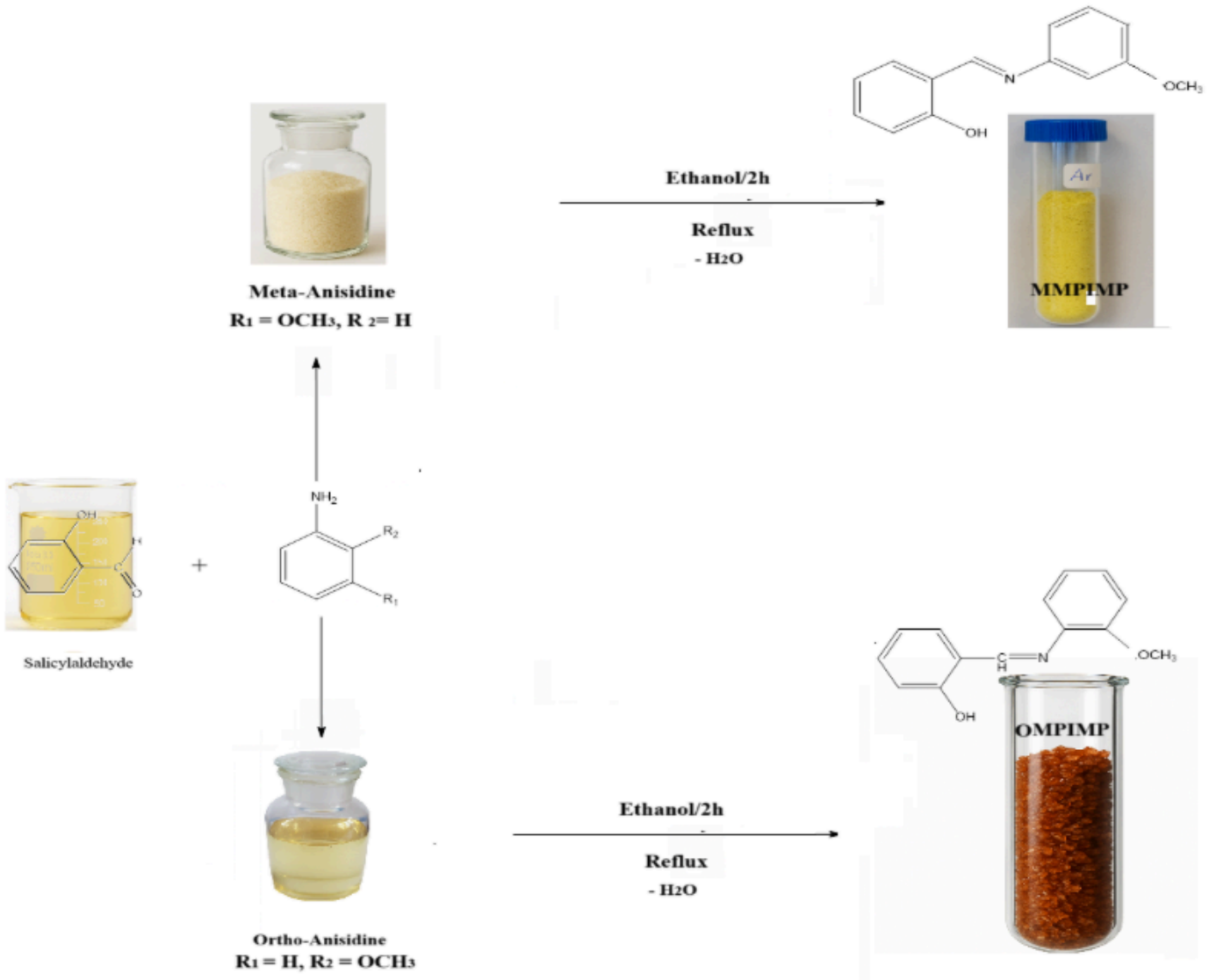


**Figure 1**

Synthesis scheme of Schiff bases.

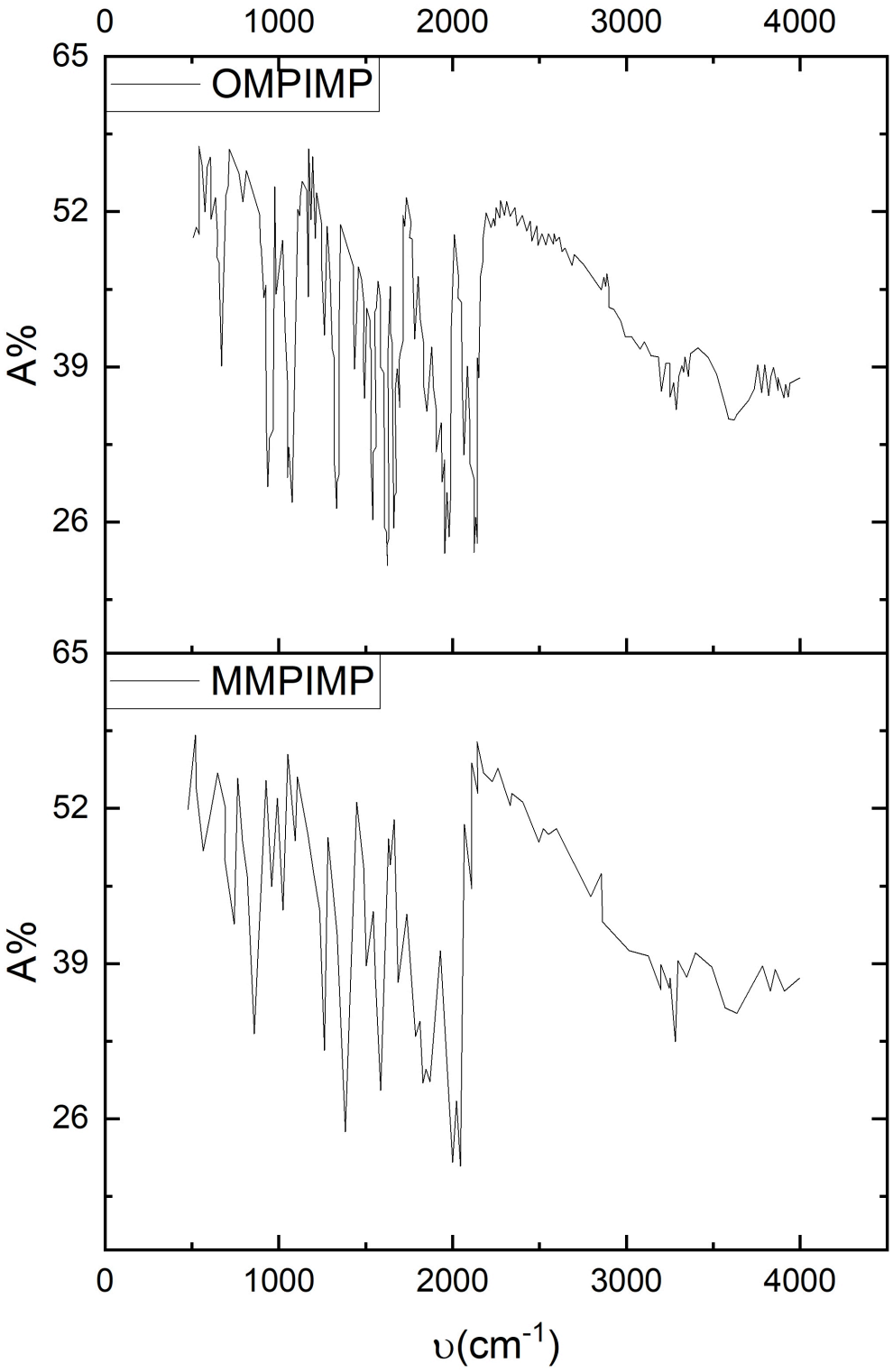



**Figure 2**

IR spectra of Schiff bases MMPIMP and OMPIMP.

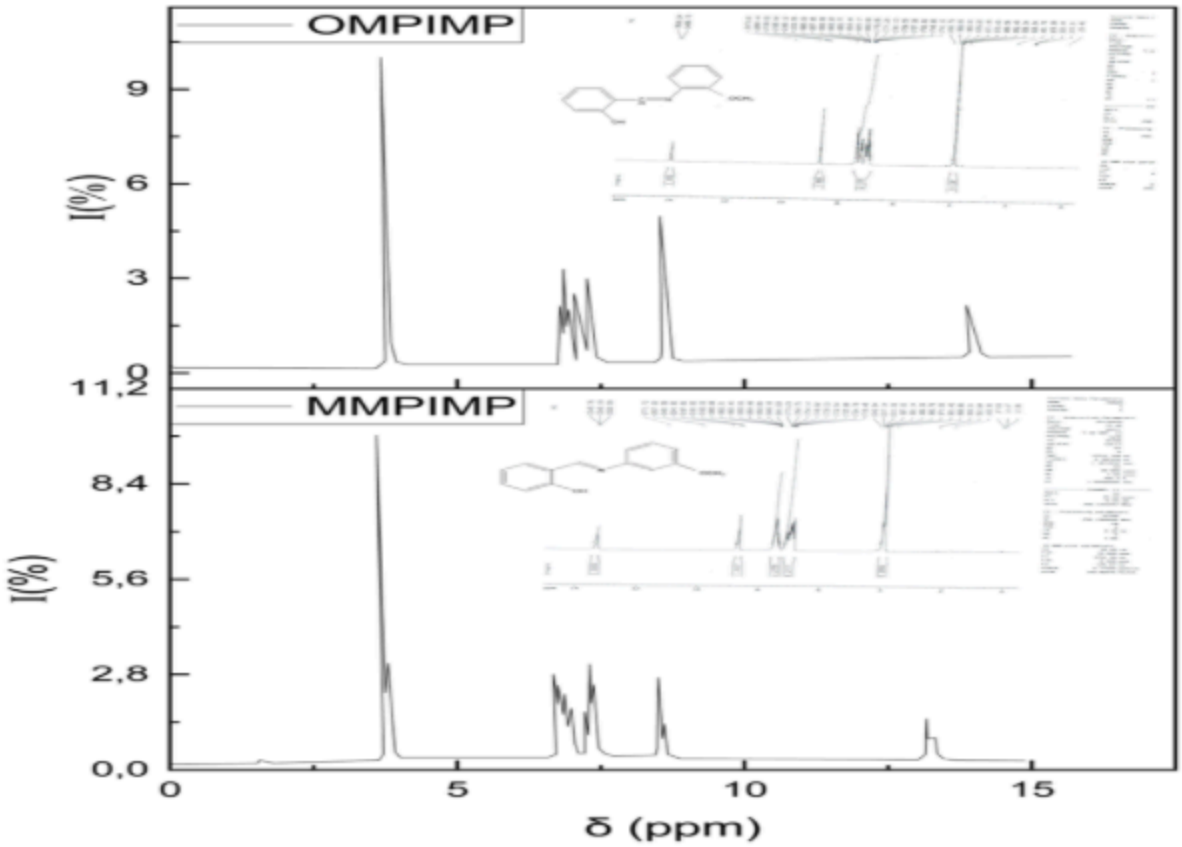



**Figure 3**

$^{1}$H NMR spectra of Schiff bases MMPIMP and OMPIMP.

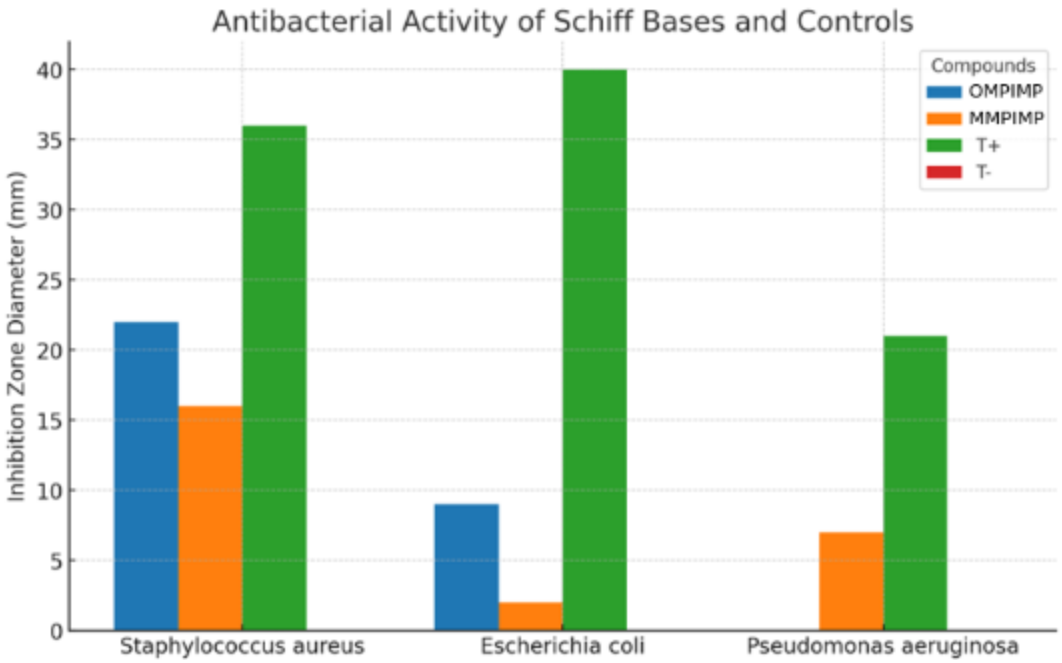



**Figure 4**

Antibacterial Activity of Schiff bases.

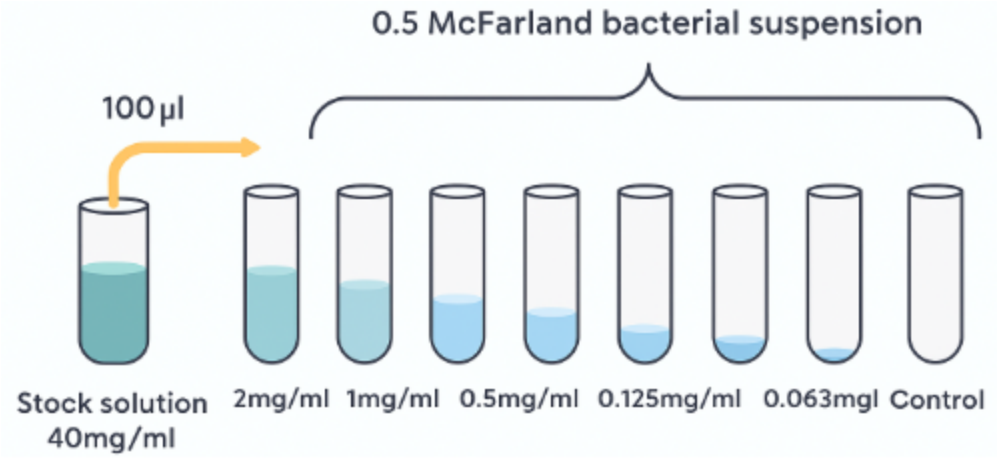



**Figure 5**

Broth Dilution Assay for Minimum Inhibitory Concentration (MIC) Determination.

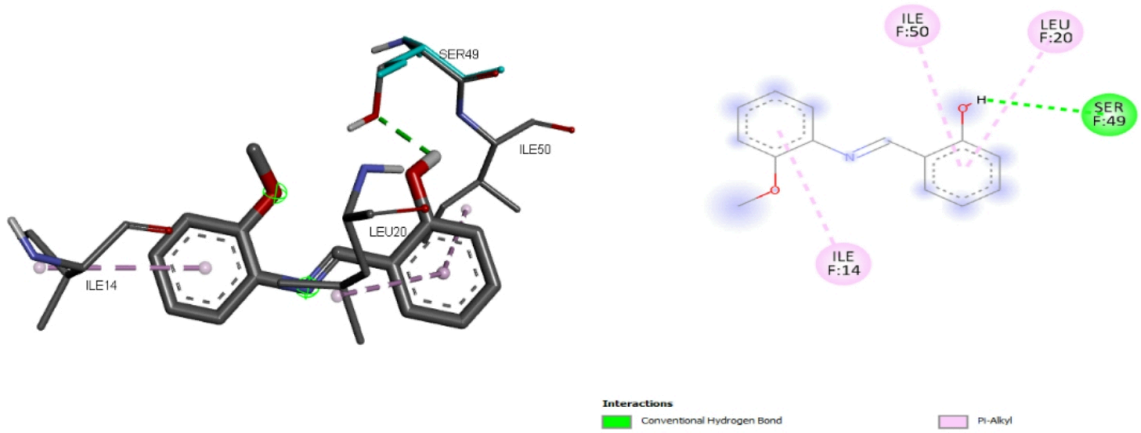



**Figure 6**

2W9S-OMPIMP interaction 2D, 3D.

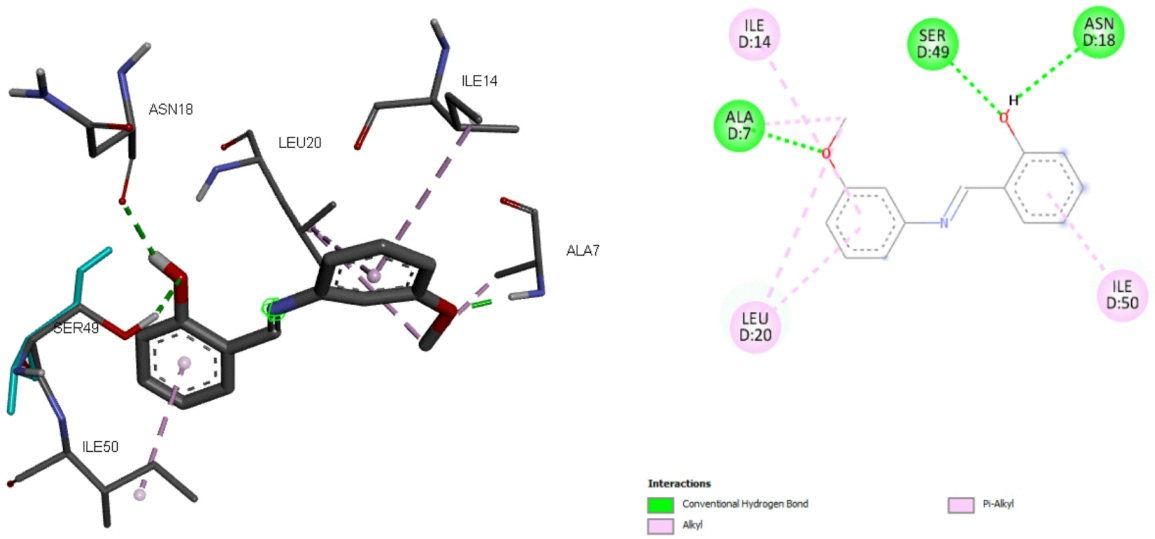



**Figure 7**

2W9S-MMPIMP interaction 2D, 3D.

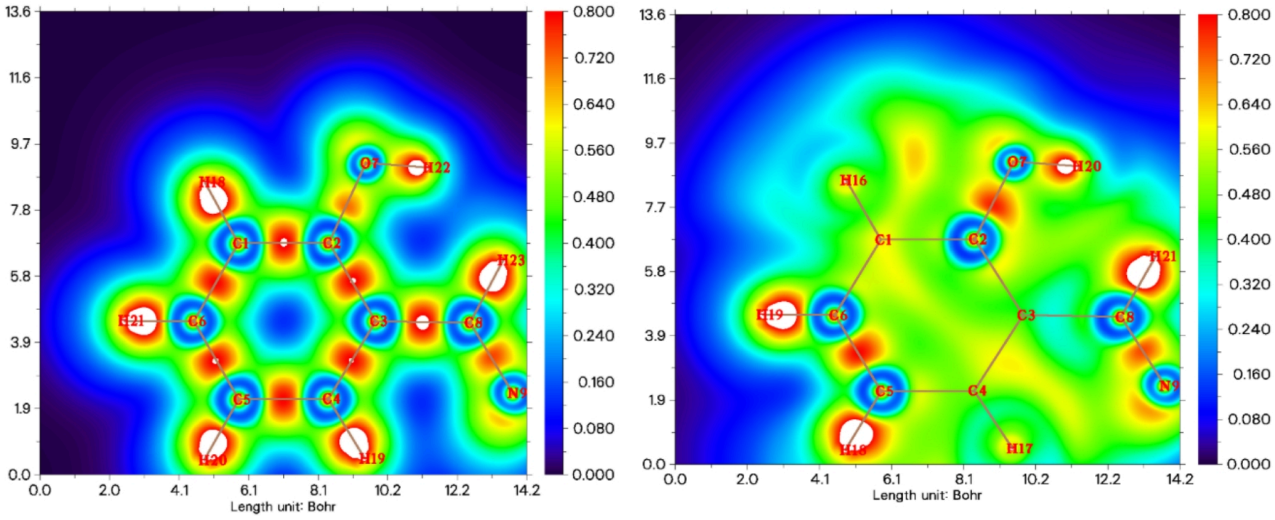



**Figure 8**

RDG Isosurface Maps for MMPIMP and OMPIMP: Visualization of Non-Covalent Interactions